

## Core-shell biopolymer microspheres for sustained drug release

Liqing Tan,<sup>1,2</sup> Tao Jiang,<sup>1,3</sup> Xiaolan Yang,<sup>4</sup> Wei Li,<sup>1</sup> Lijun Pan,<sup>5</sup> Mingan Yu<sup>1</sup>

<sup>1</sup>Department of Medicinal Chemistry, School of Pharmacy, Chongqing Medical University, Chongqing 400016, People's Republic of China

<sup>2</sup>Department of Pharmacy, The Third Affiliated Hospital of Third Military Medical University, Chongqing 400042, People's Republic of China

<sup>3</sup>Department of Pharmacy, Xinqiao Hospital of Third Military Medical University, Chongqing 400037, People's Republic of China

<sup>4</sup>Key Laboratory of Clinical Laboratory Diagnostics of the Education Ministry, College of Laboratory Medicine, Chongqing Medical University, Chongqing 400016, People's Republic of China

<sup>5</sup>Pharmaceutical Teaching Laboratory, Chongqing Medical University, Chongqing 400016, People's Republic of China

Liqing Tan, Tao Jiang, and Xiaolan Yang contributed equally to this work.

Correspondence to: M. Yu (E-mail: minganyu666@outlook.com)

**ABSTRACT:** In this work, a core-shell biopolymer microsphere comprising a carvedilol-loaded yeast cell wall polysaccharides core surrounded by a silk fibroin shell layer is developed to eliminate the risks of using synthetic polymers for drug encapsulation on human health and to avoid burst release and to prolong the release time. Transmission electron microscopy, Fourier-transform infrared, confocal laser scanning microscope, and phase contrast microscopy analysis indicate that yeast treated with Tris-HCl containing cetyltrimethylammonium bromide, EDTA, and NaCl could provide much larger space for host drug as compared to plasmolyzed cells because the former can help maintain the original shape of yeast cells. In addition, its permeability barrier is significantly altered and nucleus becomes pyknotic. In contrast, plasmolyzed cells can hardly maintain the rigidity and integrity of their cell walls and will finally end up with cell fragments. SEM observation reveals that the carvedilol-loaded cells maintain very similar shape and size before and after coating with 0.1% silk fibroin. *In vitro* release studies show that a drug delivery system using the carvedilol-loaded cells can achieve a sustained drug release up to 20 days probably due to the electrostatic interaction between the positively charged carvedilol and the negatively charged yeast cells at the pH 7.4 and to the stability of the yeast cell helped by silk fibroin that provides an effective diffusion barrier. © 2014 Wiley Periodicals, Inc. *J. Appl. Polym. Sci.* **2015**, *132*, 41782.

**KEYWORDS:** brewer's yeast; cetyltrimethylammonium bromide; core-shell biopolymer microspheres; drug delivery systems; silk fibroin

Received 14 July 2014; accepted 20 November 2014

**DOI:** 10.1002/app.41782

### INTRODUCTION

In recent 20 years, core-shell microspheres, also known as double-walled microspheres, with a drug-encapsulating particle core surrounded by a drug-free shell layer have attracted considerable attention thanks to their outstanding properties and their promising applications in the pharmaceutical and medical fields. Nevertheless, most of them are made of poly(lactic-co-glycolic acid) (PLGA) and poly(lactide) (PLA).<sup>1–13</sup> Although PLGA and PLA are FDA-approved biodegradable macromolecules,<sup>14</sup> due to their high hydrophobic nature, the polymers need to be dissolved in an organic solvent, usually methylene chloride, chloroform, or ethyl acetate,<sup>1,10–13</sup> which are undesirable for safety and environmental reasons.<sup>15,16</sup> Moreover, the acidic by-products from their degradation can reduce the local solution pH and cause inflammatory responses and foreign body

reactions *in vivo*.<sup>17,18</sup> Therefore, alternative approaches are needed for the preparation of core-shell microspheres.

Yeast-based microencapsulation technology has progressed well in food, agrochemicals, cosmetics, and pharmaceuticals as yeast cell envelope is a natural “preformed” capsule, with a lipid bilayer membrane and an outer cell wall that consists of a  $\beta$ -1,3-glucan (ca. 60% of the cell wall dry mass) network, a mannoprotein (ca. 40% of the cell wall dry mass) layer, and a small amount of chitin (ca. 2% of the cell wall dry mass), the double carbohydrate wall/lipid membrane capsule prevents volatile products from evaporation, and damage from light, oxidation, and excessive heat, therefore, providing a highly stable product with extended shelf-life. Moreover, it is cost-effective against all known microencapsulation technology.<sup>19,20</sup> So a hollow, porous micrometer-sized baker's yeast shells composed primarily of  $\beta$ -

1,3-D-glucan has recently been prepared by treating baker's yeast with high concentration of sodium chloride or a series of sodium hydroxide, hydrochloric acid, and solvent extractions, and has been used as factories for the encapsulation of both hydrophobic and hydrophilic molecules such as resveratrol,<sup>21</sup> DNA,<sup>22</sup> siRNA,<sup>23</sup> and curcumin.<sup>24</sup> However, it is well known that both hydrochloric acid and sodium hydroxide are extremely corrosive, and can probably disrupt the yeast cells.<sup>25</sup> Moreover, high sodium chloride concentrations may also have a negative impact on the integrity and potency of biologicals.<sup>26</sup> Fortunately, a new technique using cytochalasin B-treated mouse fibroblasts (3T3 cells) or human embryonic kidney cells (HEK293 cells) as factories has been developed to produce cell membrane capsules in the size range of cells. Although this technique has achieved the first success in encapsulation of drugs and nanoparticles,<sup>27</sup> it costs far more than that of yeast cells.

In our previous report, cetyltrimethylammonium bromide (CTAB) permeabilized brewer's yeast cells have been successfully used as the whole cell biocatalysts for the synthesis of chiral alcohols, in which permeability barrier of the cell membrane to substrates and/or products has been significantly reduced by the permeabilization treatment.<sup>28</sup> In addition, the earlier work indicated that permeabilized cellular geometric relationships and protein concentrations were similar to those of living cells.<sup>29</sup> In this study, we use brewer's yeast treated with Tris-HCl containing CTAB mixtures as production workshop to manufacture cell wall polysaccharides core for encapsulation of drugs, which was then coated with silk fibroin (SF) to avoid burst release and prolong the release time.<sup>21</sup>

The morphologies and characteristics of yeast cells untreated and treated with sodium chloride, alkaline/acid, and Tris-HCl containing CTAB mixtures were investigated using transmission electron microscopy, Fourier infrared transmission spectroscopy, and phase contrast microscopy to compare their similarities, differences, and analyze their feasibilities as core materials. The cell permeability was examined by encapsulation of rhodamine B in yeast cell wall polysaccharides, followed by observing fluorescence using confocal laser scanning microscope. The *in vitro* drug release of the core-shell microspheres formed by SF coatings on the drug-loaded brewer's yeast was studied and the morphology before and after drug release was investigated by scanning electron microscope.

## EXPERIMENTAL

### Materials

Cocoons of *Bombyx mori* silkworm silk were kindly supplied by China National Silk Museum (Hangzhou, China). Carvedilol with purity of 99.3% was obtained from Adamas Reagent (Shanghai, China). CTAB was purchased from Chengdu Kelong Chemical Reagent Factory (Chengdu, China). Rhodamine B (RhB) was acquired from China National Pharmaceutical Group Corporation, Shanghai Chemical Reagents Company (Shanghai, China). Other chemicals used were of reagent grade except where noted.

### Brewer's Yeast and Pretreatment

Fresh brewer's yeast slurry (a strain of *Saccharomyces cerevisiae*), a by-product from brewery with a solids content of about 20%,

was purchased from Chongqing Beer Group (Chongqing, China). The fresh yeast cells were harvested by centrifugation at 3000 rpm for 10 min. The yeast pellet was again diluted two to three times with 0.9% NaCl (saline) at 0–2°C, screened on a 100 mesh screen and centrifuged at 5000 rpm for 30 min, and then permeabilized as previously described<sup>28,30</sup> or plasmolyzed with 10% (w/v) sodium chloride solution<sup>24</sup> or with a series of sodium hydroxide, hydrochloric acid, and solvent extractions.<sup>22,23</sup> Nevertheless, 0.2% (w/v) CTAB permeabilization solution was replaced with 0.01M Tris-HCl, pH 7.0 containing 0.2% (w/v) CTAB, 0.1M EDTA tetrasodium salt, and 0.02M sodium chloride.<sup>31,32</sup> Finally, the untreated and the treated cells were again centrifuged, washed twice with distilled water, and then freeze-dried.

### Feasibility Analysis of Brewer's Yeast as Core Material

The untreated, permeabilized, and plasmolyzed cells were evaluated for their morphology, membrane integrity, permeability for Rhodamine B, and drug loading capacity. The cell morphology was observed using transmission electron microscopy (TEM). Samples were prepared by treating the freeze-dried cells with 3.6% glutaraldehyde in 0.1M phosphate buffer, pH 7.2, at 4°C for 2 h, and postfixed with OsO<sub>4</sub> in the same buffer. Then, the treated cells were dehydrated with sequential ethanol concentrations (30–100%), and embedded in Epon 812 for 48 h. Sectioning was performed using an Ultracut E microtome, and sections were post-stained with uranyl acetate and lead citrate before being studied by TEM model JEOL122 at 80 kV (Tokyo, Japan).

The untreated and treated yeast cells were also analyzed by the Fourier-transform infrared (FTIR), model 5DXC Nicolet, Madison, WI. Each sample was prepared by KBr disk method and scanned 64 times from 500 to 4000 cm<sup>-1</sup> with a resolution of 4 cm<sup>-1</sup>.

To evaluate the cell permeability, 10 mg of freeze-dried yeast cells were dispersed in 10 mL of distilled water to form a suspension. Suspension (1 mL) was added to 0.2% (w/v) (1 mL) rhodamine B aqueous solution and mixed well, and then kept in dark for 4 h. The mixture was then centrifuged at 10,000 rpm for 15 min. After decanting the supernatant solution, the cells were rinsed with ice-cold PBS for three times, and treated with fresh 4% (w/v) paraformaldehyde for 20 min at room temperature. The cells were studied using a Zeiss LSM 510 confocal laser scanning microscope (Carl Zeiss, Oberkochen, Germany).

In addition, freeze-dried yeast cells were also dispersed in distilled water to form a suspension and the pyknosis was then studied by a phase contrast light microscope (Carl Zeiss, Jena, Germany) equipped with a Sony Exwave HAD 3CCD color video camera.

### Preparation of Carvedilol-Loaded Brewer's Yeast Microcapsules

To prepare microcapsules loaded with carvedilol in brewer's yeast core, 120 mg of carvedilol was dissolved in 75 mL of absolute ethyl alcohol and vortexed for 60 s. The resulting solution was slowly added into 75 mL of 0.5% (w/v) cells suspension

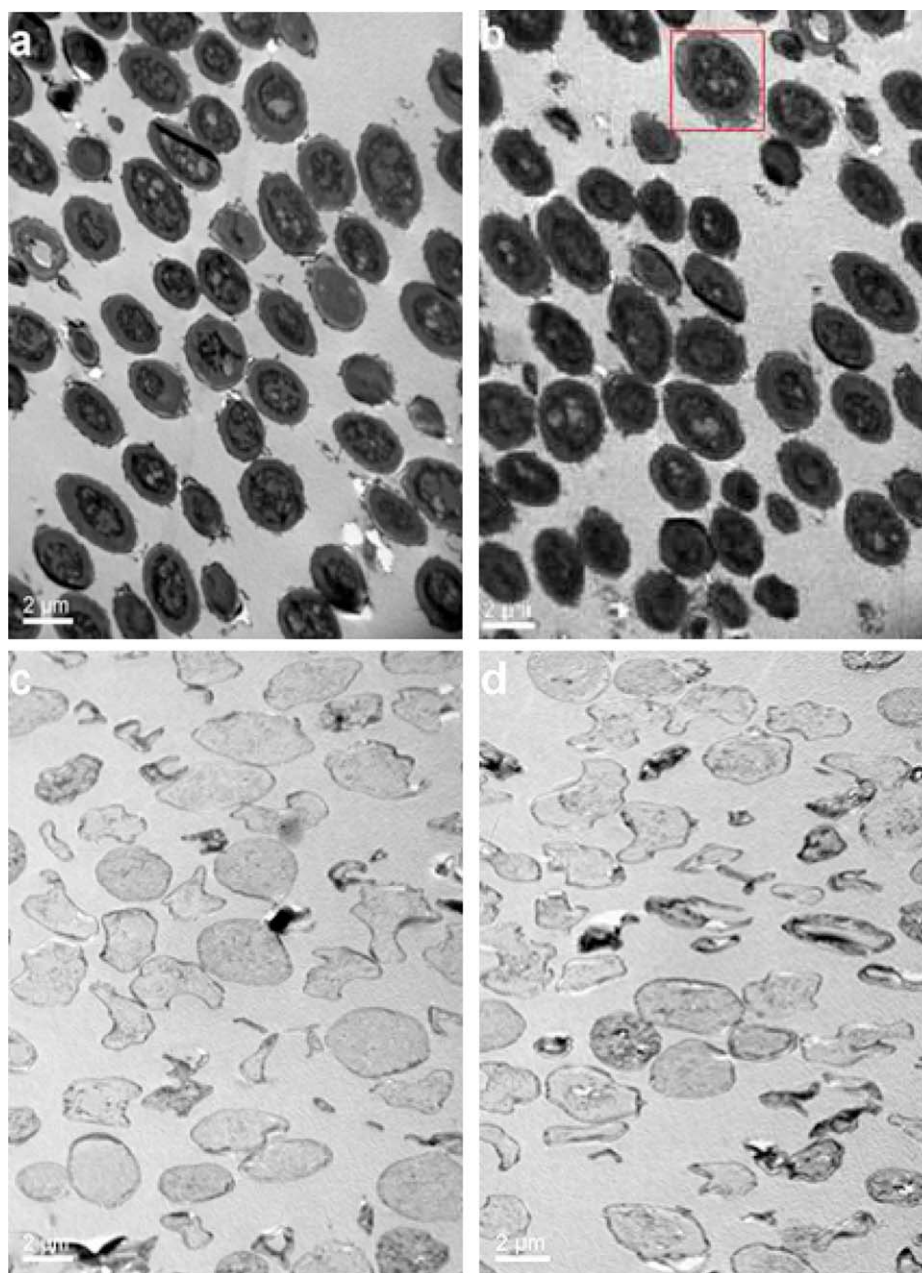


**Figure 1.** TEM images of brewer's yeast untreated (a) and treated with 0.01M Tris-HCl, pH 7.0 containing 0.2% (w/v) CTAB, 0.1M EDTA tetrasodium salt, and 0.02M sodium chloride (b), 10% (w/v) sodium chloride (c), and a series of sodium hydroxide, hydrochloric acid, and solvent extractions (d). [Color figure can be viewed in the online issue, which is available at [wileyonlinelibrary.com](http://wileyonlinelibrary.com).]

under gentle stirring at a rate of 60 mL/h and allowed to equilibrate for another 7 h at 40°C. The mixture was then sonicated for 30 s at 25 W output. The resulting microcapsules were then centrifuged at 4000 rpm for 15 min to remove free carvedilol and freeze-dried for 48 h. The absorbance of free drug in the supernatant was measured by UV-vis spectrophotometry (V-630, Jasco) at 240 nm and the drug concentration was calculated based on the absorbance spectrum. Weight of carvedilol in cells was determined by the difference between the carvedilol added and remained in the supernatant. Thus, the drug loading capability (LC) of the cell microcapsules was calculated using the following formulae<sup>33</sup>:

$$LC (\%) = \frac{\text{weight of carvedilol in cells}}{\text{weight of cells}} \times 100\%.$$

#### Silk Fibroin Coating

SF aqueous stock solutions were prepared as described previously.<sup>34</sup> Briefly, cocoons of *B. mori* were boiled two times for 1 h in an aqueous solution of 0.02M sodium carbonate and rinsed thoroughly with water. The extracted SF was dissolved in 9M LiBr solution to obtain a 10% (w/v) solution. This solution was dialyzed against water for 2.5 days using Slide-a-Lyzer dialysis cassettes (MWCO 3500, Pierce) to remove the salt. The resulting solution was centrifuged to remove impurities and



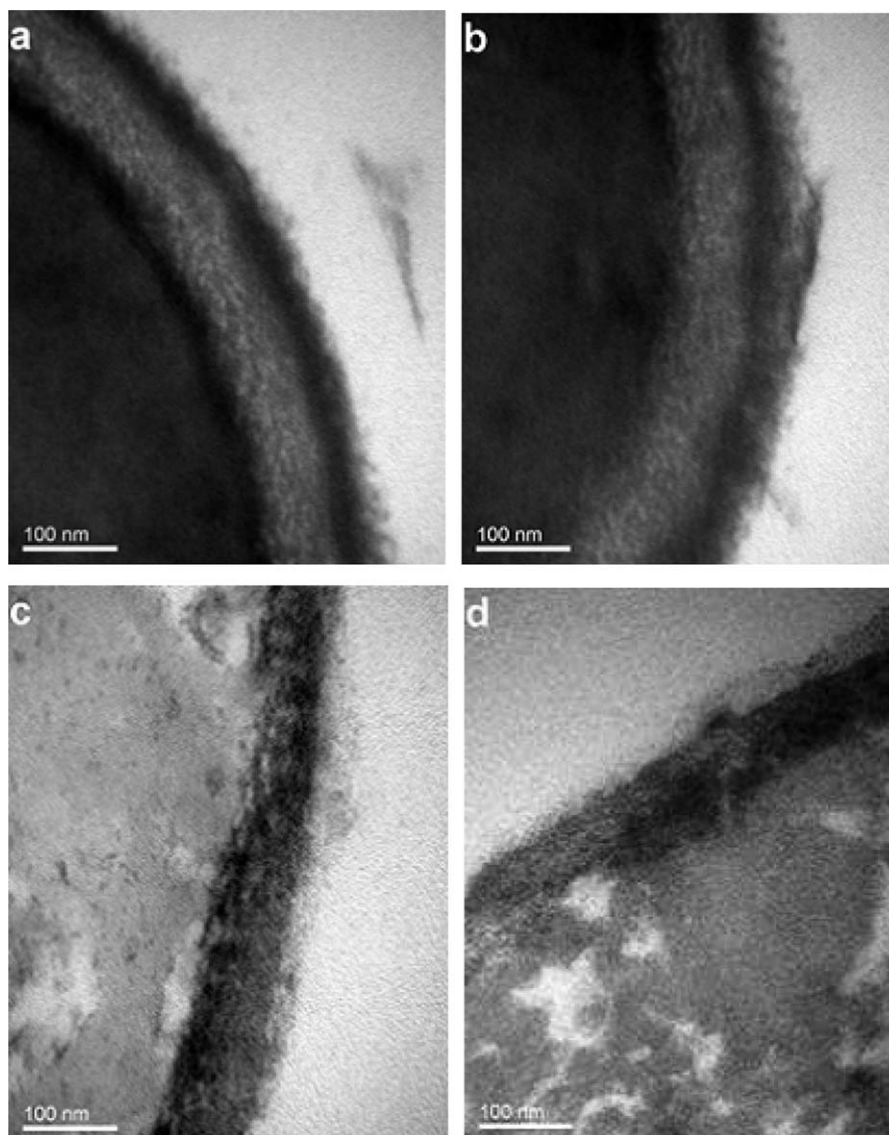


**Figure 2.** High-resolution TEM images of brewer's yeast cell wall untreated (a) and treated with 0.01M Tris-HCl, pH 7.0 containing 0.2% (w/v) CTAB, 0.1M EDTA tetrasodium salt, and 0.02M sodium chloride (b), 10% (w/v) sodium chloride (c), and a series of sodium hydroxide, hydrochloric acid, and solvent extractions (d).

aggregates that were formed during dialysis. The final concentration of silk fibroin aqueous solution was approximately 8% (w/v). This concentration was determined by weighing the residual solid of a known volume of solution after drying. Silk solutions used for coating formation were prepared by diluting the stock silk solution with distilled water to a concentration (in w/v) of 0.1%, 0.2%, and 0.3%, respectively. Surface coating of carvedilol-loaded brewer's yeast microcapsules is achieved by electrostatic layer-by-layer assembly techniques between CTAB<sup>31,35</sup> and SF.<sup>34</sup> Briefly, 0.3 g of carvedilol-loaded cell microcapsules were suspended in 10 mL of 0.2% (w/v) CTAB aqueous solution. The suspensions were sonicated for 30 s to ensure uniform mixing and gently shaken for 2 min at room temperature, followed by the free CTAB was removed by centrifugation for 5 min at 10,000 rpm. The obtained microspheres were dried by a gentle flow of dry nitrogen gas, and then immersed in the SF aqueous solution and sonicated

for 30 s, followed by gently shaken for 2 min at room temperature. To remove free SF, the microspheres suspension was centrifuged for 5 min at 10,000 rpm, and then the microspheres were dried by a gentle flow of dry nitrogen gas. The resulting microspheres were again coated with CTAB and SF, respectively. The above procedures were repeated three times to get the silk-coated core-shell microspheres. SEM images of the microspheres were obtained using an S-3000N instrument (Hitachi, Japan). The SEM sample was prepared by dispersing the microspheres in distilled water and dropped onto freshly cleaved cover glass, and then dried at 60°C. Subsequently, a few nm thick layer of gold was sputtered onto the surface of cover glass prior to imaging.

#### **In Vitro Release Studies**

*In vitro* release study was conducted in PBS.<sup>11,34</sup> Briefly, 100 mg of the dried samples was dispersed into 10 mL of PBS, of which

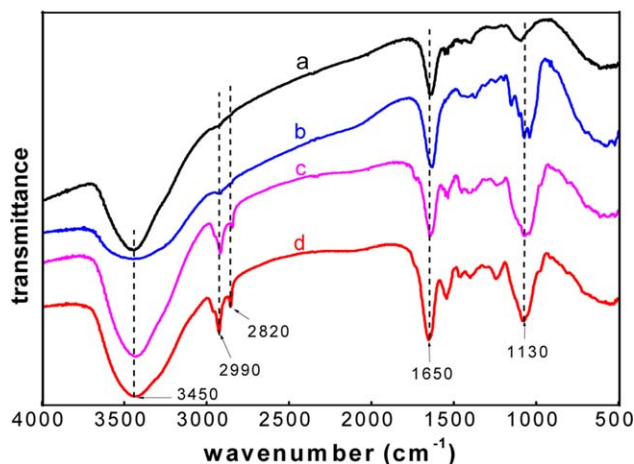


**Figure 3.** FTIR spectra of brewer's yeast untreated (a) and treated with 0.01M Tris-HCl, pH 7.0 containing 0.2% (w/v) CTAB, 0.1M EDTA tetrasodium salt, and 0.02M sodium chloride (b), 10% (w/v) sodium chloride (c), and a series of sodium hydroxide, hydrochloric acid, and solvent extractions (d). [Color figure can be viewed in the online issue, which is available at [wileyonlinelibrary.com](http://wileyonlinelibrary.com).]

0.5 mL of the mixture was collected and placed into dialysis tubing, well immersed in the 30 mL PBS at a pH of 7.4. The tubes were then incubated in a water-bath shaker at 37°C with continuous shaking at 120 rpm. Release medium (1.0 mL) was withdrawn at predetermined time intervals and replaced with fresh PBS. All measurements were performed in triplicate ( $n = 3$ ). The samples were analyzed by UV-vis spectrophotometry at 240 nm as applied for LC determination. The percentage of drug released at each time point was calculated using the following formulae:

$$\text{Drug release (\%)} = \frac{\text{Carvedilol in supernatant } (\mu\text{g/mL})}{\text{Initial carvedilol in microspheres } (\mu\text{g/mL})} \times 100\%.$$

### Statistical Analysis

All values were expressed as means  $\pm$  standard deviation (SD). Statistical data analyses were performed using a one-way ANOVA (Origin Pro 9.0) for  $n = 3$ . A difference of  $P < 0.05$  was considered statistically significant.

## RESULTS AND DISCUSSION

### Cell Morphology

For a better understanding of the morphological effect of environmental changes on brewer's yeast, the cells were, respectively, treated with and without sodium chloride, alkaline/acid, and Tris-HCl containing CTAB mixtures, and then observed by TEM. As shown in Figure 1, the cells with different treatment strategies exhibited a completely different morphology. More specifically, untreated cells showed well preserved morphology in size and shape [Figure 1(a)] and the cells treated with CTAB [Figure 1(b)] were similar to untreated ones as well. This is in agreement with the previous study<sup>25</sup> which indicated that the wall/cell membrane can be permeabilized with 0.2% (w/v) CTAB without the fragmentation of the cells. However, the cells treated with sodium chloride or acid/alkaline showed severe deformation and fragmentations [Figure 1(c,d)]. We believe this

is due to the damages and disruptions of the glycosidic linkage in the cell skeleton.

It is well-known that at the non-reducing ends of the 1,3- $\beta$ -glucan molecules in the yeast cell wall, highly branched 1,6- $\beta$ -glucan chains are linked together by glycosidic linkages, while at the inside of the 1,3- $\beta$ -glucan network in the lateral walls, chitin is covalently linked through its reducing end to 1,3- $\beta$ -glucan and 1,6- $\beta$ -glucan.<sup>36</sup> To prepare hollow, porous micrometer-sized shells composed primarily of  $\beta$ 1,3-glucan through treating baker's yeast with a series of alkaline, acid, and solvent extractions by remove other cell wall polysaccharides,<sup>23</sup> the glycosidic linkages of the covalent link to  $\beta$ 1,3-glucan network must be broken so that 1,6- $\beta$ -glucan and chitin are free to pulling away from the cell wall. Unfortunately, the break of chemical bond is in general random and not specific to any one glycosidic linkage and the internal  $\beta$ 1,3-linkages in 1,3- $\beta$ -glucan can also break, resulting in the weakening of the cell walls that finally would break into cell fragments [Figure 1(c,d)]. Therefore, these cells are not usable for core material until they are permeabilized.

Indeed, it can be seen more clearly from high-resolution TEM, as shown in Figure 2, that the untreated cells have smooth and intact surface morphology [Figure 2(a)], while the walls of the cells treated with both sodium chloride and alkaline/acid were seriously damaged or destroyed [Figure 2(c,d)]. The lack of structural integrity in the walls of the treated cell is a direct evidence that the 1,3- $\beta$ -glucan network is cleaved under the environmental stresses. We can also see that their plasma membranes have been seriously damaged as well. On the contrary, cell wall and plasma membranes of brewer's yeast have only small changes with no fragmentation after treatment with CTAB [Figure 2(b)]. These results further demonstrated that the CTAB-permeabilized cells should be far more efficient and reliable as a core material for drug encapsulation than plasmolyzed cells.

### Characterization of Brewer's Yeast

FTIR was used to further estimate whether permeation or plasmolysis had modified the structure of the membrane. As shown in Figure 3, the absorption peak associated with hydroxyl groups (a broad band in the range 3500–3200  $\text{cm}^{-1}$ ), carbonyl group ( $\sim 1650 \text{ cm}^{-1}$ ), and asymmetric stretching of the glycosidic linkages ( $\sim 1130$ ) of the chemically treated yeast cells were increased, in agreement with previous report,<sup>37</sup> there are considerable differences between the spectra of plasmolyzed, CTAB-permeabilized, and untreated cells. The most notable spectral changes were found in the 2990–2820  $\text{cm}^{-1}$  regions mainly associated to the asymmetric and symmetric stretch of  $\text{CH}_3$  and  $\text{CH}_2$  from lipids.<sup>38</sup> Obviously, the lipid absorption of the cells treated with sodium chloride [Figure 3(c)] or with alkaline/acid [Figure 3(d)] strongly increased as compared to untreated cells [Figure 3(a)]. These variations are probably related to the biochemical changes resulting from the disorganization of membrane systems, particularly of the plasma membrane.<sup>38</sup> The lipid absorption of CTAB-permeabilized cells has only slight changes [Figure 3(b)], indicating that the plasmatic membrane has not been disrupted, which is consistent with the TEM observations.

The effect of different stress conditions on the permeability of brewing yeast was visualized by staining with rhodamine B. It

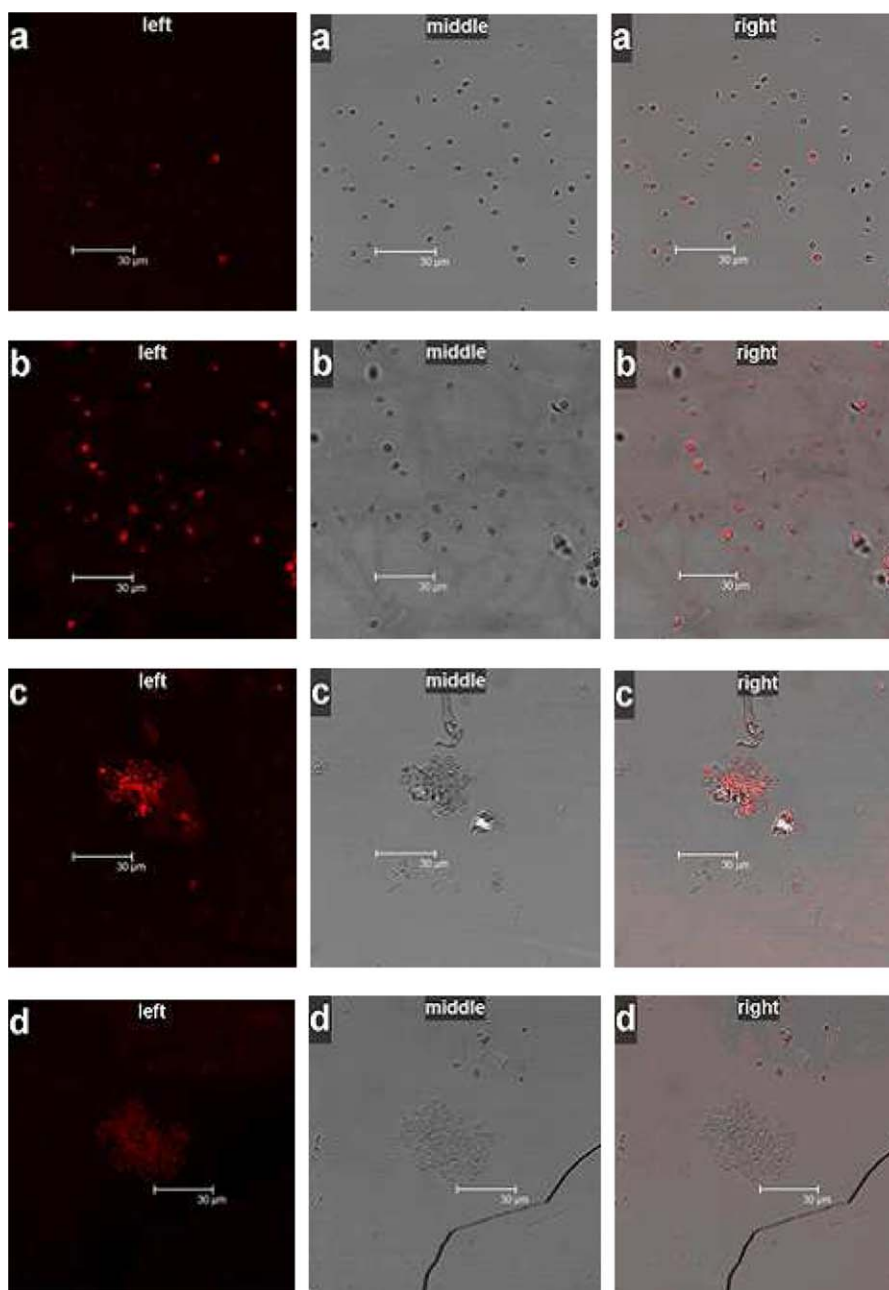


**Figure 4.** Confocal (left), brightfield (middle), and overlapped (right) micrographs of rhodamine B-loaded brewer's yeast *untreated* (a) and treated with 0.01M Tris-HCl, pH 7.0 containing 0.2% (w/v) CTAB, 0.1M EDTA tetrasodium salt, and 0.02M sodium chloride (b), 10% (w/v) sodium chloride (c), and a series of sodium hydroxide, hydrochloric acid, and solvent extractions (d) (scale bar: 30 μm). [Color figure can be viewed in the online issue, which is available at [wileyonlinelibrary.com](http://wileyonlinelibrary.com).]

was found that only a few untreated yeast cells display red fluorescence in the confocal micrograph [Figure 4(a)] while the cells treated with CTAB have the highest fluorescence, penetrating deep into yeast cells and the cells are intact [Figure 4(b)]. Although sodium chloride-treated cells also exhibit a strong fluorescence, many of them have been broken into the cell fragments and aggregated together [Figure 4(c)]. The cells treated with a series of alkaline, acid, and solvent extractions display the lowest fluorescence signal, almost invisible in most wide field imaging systems [Figure 4(d)]. These results intuitively

indicate that cell membrane permeabilization is indeed achieved by treating yeast with 0.2% (w/v) CTAB, thereby rhodamine B can be uploaded through their cell membranes and enters rapidly into the inner regions of the cell by passive diffusion. This observation is consistent with previously reported study that rhodamine 6G can effectively be encapsulated in cell membrane capsules (CMCs),<sup>27</sup> and damaged cells can cause either alkaline, acid, or solvent extractions and sodium chloride is no longer able to accumulate significant amounts of rhodamine B. Based on the above analysis we come to a conclusion that CTAB-



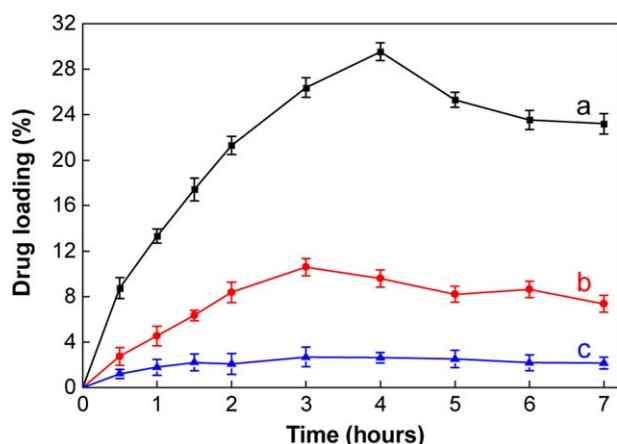


**Figure 5.** Carvedilol-loading capability (LC) of brewer's yeast. Cells treated with 0.01M Tris-HCl, pH 7.0 containing 0.2% (w/v) CTAB, 0.1M EDTA tetrasodium salt, and 0.02M sodium chloride (a), 10% (w/v) sodium chloride (b), and a series of sodium hydroxide, hydrochloric acid, and solvent extractions (c). Each point represents the mean  $\pm$  SD ( $n = 3$ ). [Color figure can be viewed in the online issue, which is available at [wileyonlinelibrary.com](http://wileyonlinelibrary.com).]

permeabilized cells are one of the best candidates for a humanized core material for preparing double-walled microspheres.

To evaluate the capability of drug loading using permeabilized yeast cells, carvedilol, a non-selective beta-blocker with  $\alpha$ -blockage, vasodilatation, and antioxidant effects, was chosen as model drug and plasmolyzed yeast cells were used as control. UV-vis spectroscopy was used in this work to monitor the incorporation of the model compounds. The results were shown

in Figure 5. Obviously, after an equilibration time of 7 h under the experimental conditions, permeabilized yeast cells showed a maximum loading of 29.3% [Figure 5(a)], which was much higher than that of the cells either with sodium chloride or a series of alkaline, acid, and solvent extractions [Figure 5(b,c)]. This revealed that permeabilized cells could indeed effectively enhance drug encapsulation. This is because that the permeability barrier of the cells was altered to enable the penetration of drug molecules not permeable through the intact cell membrane while the cells still remained spherical in shape like untreated cells [Figure 6(a)], but with a pyknotic instead of nucleus [Figure 6(b)]. Pyknosis is the result of chromatin condensation and is visible by light microscopy.<sup>39</sup> The pyknotic cells have a high density of nuclear material that is uniformly and aggregate in some areas of the nucleus, while the cell membrane remains intact [Figure 2(b)], thus provided a good encapsulation workshop, promoting drugs retention. Nevertheless, from the biological perspective, pyknotic cells may undergo initial stages of apoptosis, in which the cell membrane remains intact. However, this theory has not been proven and the precise biological significance of pyknotic cells is unclear.<sup>32,40</sup> In contrast to permeabilized yeast, most of plasmolyzed cells are seriously damaged and densely aggregated together [Figure 6(c,d)] in the treatment process. These cells have lost their integrity and lysis occurs, thus it is difficult to enclose drug in these cells with acceptable drug loading capacity [Figure 5(b,c)].<sup>21-23</sup>

#### Silk Fibroin Coating and *In Vitro* Drug Release Profiles

Ideally, the drug delivery vehicles should be able to efficiently load high weight fraction of drugs. Because the carvedilol

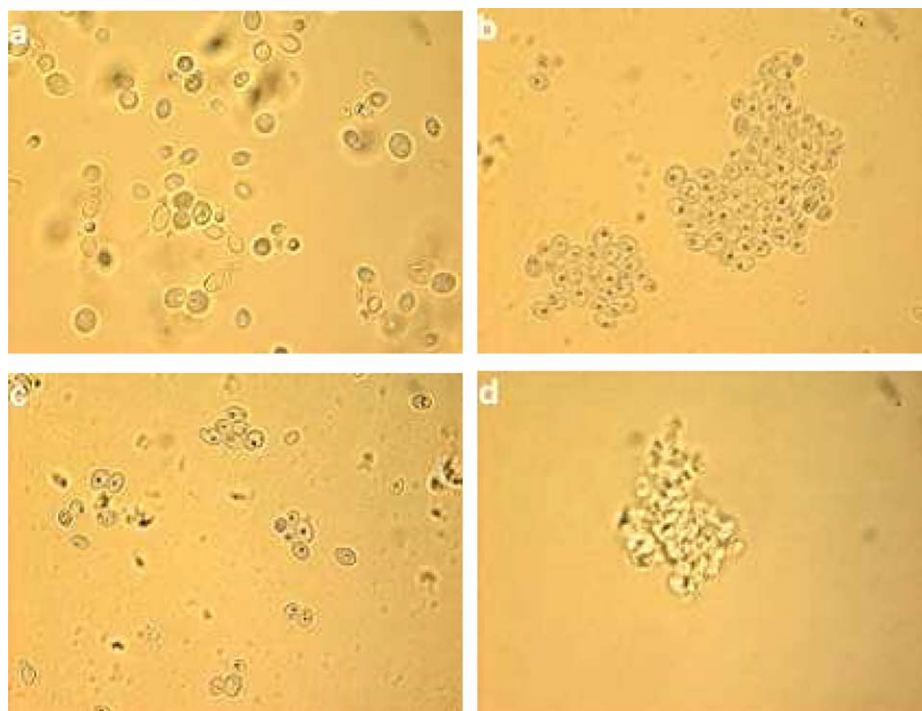


**Figure 6.** Phase-contrast micrographs of brewer's yeast untreated (a) and treated with 0.01M Tris-HCl, pH 7.0 containing 0.2% (w/v) CTAB, 0.1M EDTA tetrasodium salt, and 0.02M sodium chloride (b), 10% (w/v) sodium chloride (c), and a series of sodium hydroxide, hydrochloric acid, and solvent extractions (d). [Color figure can be viewed in the online issue, which is available at [wileyonlinelibrary.com](http://wileyonlinelibrary.com).]

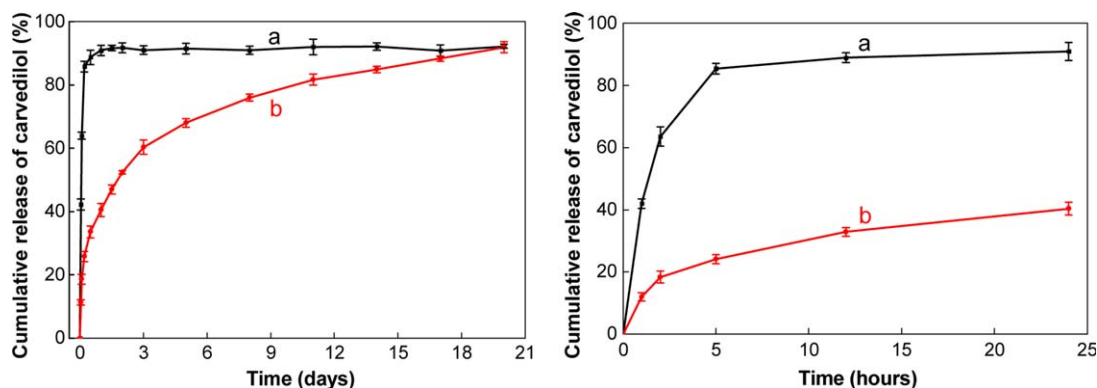


**Figure 7.** Cumulative percentage of drug release. (a) Carvedilol-loaded brewer's yeast and (b) carvedilol-loaded yeast cells were coated with CTAB/SF. Cells were treated with 0.01M Tris-HCl, pH 7.0 containing 0.2% (w/v) CTAB, 0.1M EDTA tetrasodium salt, and 0.02M sodium chloride. The CTAB/SF rate was (w/v %): 0.2 : 0.1. The right figure shows the initial release profiles within the first 24 h. Each point represents the mean  $\pm$  SD ( $n = 3$ ). [Color figure can be viewed in the online issue, which is available at [wileyonlinelibrary.com](http://wileyonlinelibrary.com).]

loading by plasmolyzed cells is quite low [Figure 5(b,c)], study on their release characteristics is not very useful. Figure 7 showed the *in vitro* drug release profiles of the carvedilol-loaded permeabilized yeast cells before and after SF coating. As shown, the yeast cells without coating exhibited a burst release of 64% within the first 2 h [Figure 7(a)] while the coated cells showed significantly retarded carvedilol release [Figure 7(b)]. The result is consistent with the results from the study by Wang *et al.* who

demonstrated that SF coatings would not only stabilize PLGA microspheres from degradation but also sustain drug release from the microspheres by providing an effective diffusion barrier.<sup>34</sup> Nevertheless, unlike the SF coating on PLGA microspheres, which was primarily driven by the hydrophobic interactions,<sup>34</sup> coating yeast cells with SF are based on the alternate deposition of oppositely charged CTAB and SF onto surfaces. SF becomes a new family of advanced biomaterials and has

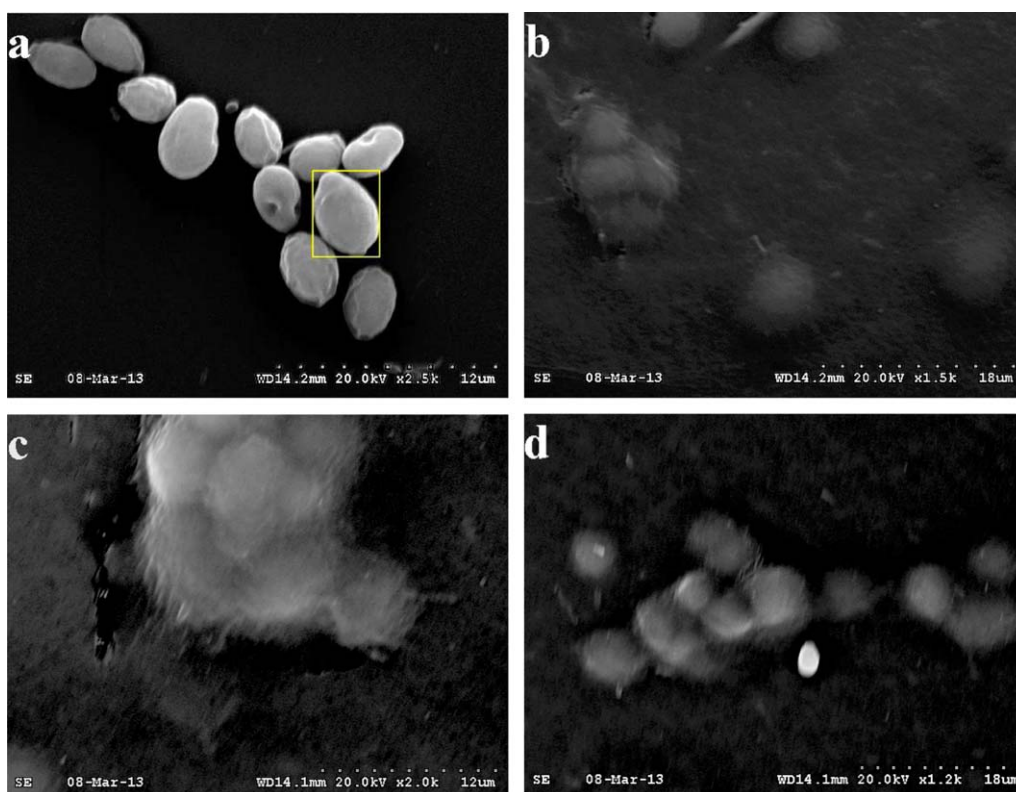


**Figure 8.** SEM images of the double-walled biopolymer microspheres consisting of a carvedilol-loaded brewer's yeast cell wall polysaccharides core surrounded by a CTAB/SF shell layer. The CTAB/SF rate was as follows (w/v %): 0.2 : 0.1 (a), 0.2 : 0.2 (b), and 0.2 : 0.3 (c). SEM image of (a) after 20 days of sustained release *in vitro* (d). The scale bar for (a) and (c) is 12  $\mu$ m while for (b) and (d) it is 18  $\mu$ m. [Color figure can be viewed in the online issue, which is available at [wileyonlinelibrary.com](http://wileyonlinelibrary.com).]



been widely used as coating materials,<sup>26,34,41</sup> thanks to its aqueous solubility, processability under very mild conditions, superior mechanical properties, and better biocompatibility both *in vitro* and *in vivo* as compared to commonly used biomaterials, such as PLA, PGA, and collagen. In drug delivery applications, CTAB is commonly used to introduce a positive surface charge to nanoparticles and has exhibited significant improvement in cellular uptake with comparison to non-modified particles.<sup>31,35</sup> As the outer surface of yeast contains numerous negatively charged groups at a  $\text{pH} \geq 3.0$ ,<sup>42</sup> the cationic head groups of the surfactant CTAB could be easily attached to the yeast cell wall by the electrostatic interactions. This electrostatic assembly then become a solid base for a negatively charged SF (SF having a pI of about 4.2)<sup>26</sup> to be absorbed on the outer layer of the CTAB-coated yeast cells. After this process was repeated three times, SEM images of the resulting microspheres are shown in Figure 8. We can see in Figure 8(a) that when 0.1% SF is used as the coating solution, the size and shape of the as-prepared microspheres are roughly the same to those of permeabilized yeast cells and there seems to have an even distribution of yeast cells with no aggregation and the microspheres have indeed a smooth outer coating of dehydrated SF-based gel layers with no observed defects or cracks. As a result, the burst release of carvedilol from the microspheres decreased by 18% within the first 2 h [Figure 7(b)]. However, after 24 h, more than 90% of carvedilol was released from the uncoated microspheres [Figure 7(a)]. In contrast, within the same time period only 40% of carvedilol was eluted from the SF-coated microspheres and a sustained release was observed over the following 19 days [Figure 7(b)]. Obviously, the results are attributed to the formation of core-shell microspheres with a core (carvedilol-loaded permeabilized yeast cells) and a second shell (a CTAB/SF-formed coat), where SF coatings not only stabilized yeast cell from aggregation and decomposition but also provided an effective diffusion barrier. Therefore, it can exhibit a reduction in the initial burst release and provide a sustained drug release. However, a slight aggregation phenomenon occurred and the resulting microspheres were covered with a thin layer of SF when the concentration of SF increased to 0.2% [Figure 8(b)]. Further increase of the SF concentration to 0.3%, the obtained microspheres come into close contact with each other and form a very dense aggregate with rough-textured surface and ill-defined interfaces, in which individual microspheres are not distinguishable [Figure 8(c)]. Therefore, the optimal coating concentration is considered to be 0.1%. The coating thickness was estimated to be approximately 0.55  $\mu\text{m}$ , which was determined by the difference between the largest microsphere with the size of approximately 5  $\mu\text{m}$  [marked in Figure 8(a) with yellow rectangle] and the largest cell with the size of approximately 3.9  $\mu\text{m}$  [marked in Figure 1(b) with red rectangle]. It is also important to note that we did not observe complete degradation of the silk coatings even after 20 days of sustained release [Figure 8(d)]. This is attributed to the superior mechanical strength and long-term degradability of the SF.<sup>26</sup>

## CONCLUSIONS

In this study, we investigated the feasibility of using brewer's yeast treated with Tris-HCl containing CTAB mixtures as work-

shop to encapsulate drug and SF as an external coating for fabricating core-shell biopolymer microspheres. Results demonstrated that the procedure can produce smooth and spherical-shaped microspheres, and their diameter is only slightly larger than that of the cells itself. More importantly, the microspheres prepared with this technique exhibit good drug loading capacity and sustained release and the SF membrane can be maintained on the cell surface for more than 20 days at neutral pH. In addition, the technique is environmental friendly, of low cost, readily available, and very easy to handle. Therefore, the as-prepared core-shell biopolymer microspheres are more promising than porous hollow micrometer-sized baker's yeast shells or traditional polymer microsphere release systems made of PLGA and PLA for medicines in the drug delivery applications.

## ACKNOWLEDGMENTS

This work was supported by the special fund of three items of expenditure on the Science and Technology department of Central District in Chongqing. The authors also thank the Chongqing Medical University for partial financial support of this work.

## REFERENCES

1. Pekarek, K. J.; Jacob, J. S.; Mathiowitz, E. *Nature* **1994**, *367*, 258.
2. Pekarek, K. J.; Jacob, J. S.; Mathiowitz, E. *Adv. Mater.* **1994**, *6*, 684.
3. Rahman, N. A.; Mathiowitz, E. *J. Control. Release* **2004**, *94*, 163.
4. Berkland, C.; Pollauf, E.; Pack, D. W.; Kim, K. *J. Control. Release* **2004**, *96*, 101.
5. Berkland, C.; Cox, A.; Kim, K.; Pack, D. W. *J. Biomed. Mater. Res. A* **2004**, *70*, 576.
6. Kokai, L. E.; Tan, H.; Jhunjhunwala, S.; Little, S. R.; Frank, J. W.; Marra, K. G. *J. Control. Release* **2010**, *141*, 168.
7. Choi, D. H.; Park, C. H.; Kim, I. H.; Chun, H. J.; Park, K.; Han, D. K. *J. Control. Release* **2010**, *147*, 193.
8. Wang, Z. *J. Appl. Polym. Sci.* **2010**, *115*, 2599.
9. Nie, H.; Fu, Y.; Wang, C. H. *Biomaterials* **2010**, *31*, 8732.
10. Zhao, H.; Wu, F.; Cai, Y.; Chen, Y.; Wei, L.; Liu, Z.; Yuan, W. *Int. J. Pharm.* **2013**, *450*, 235.
11. Xiao, C. D.; Shen, X. C.; Tao, L. *Int. J. Pharm.* **2013**, *452*, 227.
12. Xia, Y.; Ribeiro, P. F.; Pack, D. W. *J. Control. Release* **2013**, *172*, 707.
13. Xu, Q. X.; Chin, S. E.; Wang, C. H.; Pack, D. W. *Biomaterials* **2013**, *34*, 1.
14. Zhang, Z.; Feng, S. S. *Biomaterials* **2006**, *27*, 4025.
15. Lippold, B.; Sutter, B. K.; Lippold, B. C. *Int. J. Pharm.* **1989**, *54*, 15.
16. Siepmann, F.; Hoffmann, A.; Leclercq, B.; Carlin, B.; Siepmann, J. *J. Control. Release* **2007**, *119*, 182.
17. Ho, M. L.; Fu, Y. C.; Wang, G. J.; Chen, H. T.; Chang, J. K.; Tsai, T. H.; Wang, C. K. *J. Control. Release* **2008**, *128*, 142.

18. Zhou, H.; Lawrence, J. G.; Bhaduri, S. B. *Acta Biomater.* **2012**, *8*, 1999.
19. Gordon, N. *Int. J. Pharm.* **2002**, *242*, 55.
20. Aguilar-Uscanga, B.; Francois, J. M. *Lett. Appl. Microbiol.* **2003**, *37*, 268.
21. Shi, G.; Rao, L.; Yu, H.; Xiang, H.; Yang, H.; Ji, R. *Int. J. Pharm.* **2008**, *349*, 83.
22. Soto, E. R.; Ostroff, G. R. *Bioconjug. Chem.* **2008**, *19*, 840.
23. Aouadi, M.; Tesz, G. J.; Nicoloso, S. M.; Wang, M.; Chouinard, M.; Soto, E. *Nature* **2009**, *458*, 1180.
24. Paramera, E. I.; Konteles, S. J.; Karathanos, V. T. *Food Chem.* **2011**, *125*, 892.
25. Cortez, D. V.; Roberto, I. C. *New Biotechnol.* **2012**, *29*, 192.
26. Wenk, E.; Merkle, H. P.; Meinel, L. *J. Control. Release* **2011**, *150*, 128.
27. Mao, Z.; Cartier, R.; Hohl, A.; Farinacci, M.; Dorhoi, A.; Nguyen, T. L.; Mulvaney, P.; Ralston, J.; Kaufmann, S. H.; Möhwald, H.; Wang, D. *Nano Lett.* **2011**, *11*, 2152.
28. Yu, M. A.; Wei, Y. M.; Zhao, L.; Jiang, L.; Zhu, X. B.; Qi, W. *J. Ind. Microbiol. Biotechnol.* **2007**, *34*, 151.
29. Paoni, N. F.; Koshland, D. E., Jr. *Proc. Natl. Acad. Sci. USA* **1979**, *76*, 3693.
30. Gowda, L. R.; Bachhawat, N.; Bhat, S. G. *Enzyme Microb. Technol.* **1991**, *13*, 154.
31. Peetla, C.; Labhasetwar, V. *Langmuir* **2009**, *25*, 2369.
32. Thomas, P.; Hecker, J.; Faunt, J.; Fenech, M. *Mutagenesis* **2007**, *22*, 371.
33. Chen, M. C.; Tsai, H. W.; Liu, C. T.; Peng, S. F.; Lai, W. Y.; Chen, S. J. *Biomaterials* **2009**, *30*, 2102.
34. Wang, X. Q.; Wenk, E.; Hu, X.; Castro, G. R.; Meinel, L.; Wang, X. Y.; Li, C. M.; Merkle, H.; Kaplan, D. L. *Biomaterials* **2007**, *28*, 4161.
35. Fay, F.; Quinn, D. J.; Gilmore, B. F.; McCarron, P. A.; Scott, C. J. *Biomaterials* **2010**, *31*, 4214.
36. Klis, F. M.; Boorsma, A.; De Groot, P. W. *Yeast* **2006**, *23*, 185.
37. Alves, A.; Caridade, S. G.; Mano, J. F.; Sousa, R. A.; Reis, R. L. *Carbohydr. Res.* **2010**, *345*, 2194.
38. Burattini, E.; Cavagna, M.; Dell'Anna, R.; Malvezzi Campeggi, E.; Monti, F.; Rossi, F.; Torriani, S. *Vib. Spectrosc.* **2008**, *47*, 139.
39. Elmore, S. *Toxicol. Pathol.* **2007**, *35*, 495.
40. Vermes, I.; Haanen, C.; Steffens-Nakken, H.; Reutelingsperger, C. A. *J. Immunol. Methods* **1995**, *184*, 39.
41. Wang, X. Y.; Hu, X.; Daley, A.; Rabotyagova, O.; Cebe, P.; Kaplan, D. L. *J. Control. Release* **2007**, *121*, 190.
42. Klis, F. M.; De Jong, M.; Brul, S.; De Groot, P. W. *J. Yeast* **2007**, *24*, 253.